



Article

Comparative Analysis of the Solid Conveying of Regrind, Virgin and Powdery Polyolefins in Single-Screw Extrusion

Kai S. Johann *, Adrian Reißing and Christian Bonten

Institut für Kunststofftechnik, University of Stuttgart, 70569 Stuttgart, Germany;
st149964@stud.uni-stuttgart.de (A.R.); christian.bonten@ikt.uni-stuttgart.de (C.B.)

* Correspondence: kai.johann@ikt.uni-stuttgart.de

Abstract: The shape and size of processed materials play a crucial role in the solid conveying characteristics of single-screw extruders. Thus, the increasing amount of plastic regrind leads to new challenges in screw extrusion. This work investigates the conveying behavior of three distinctly different material shapes in an axially as well as a helically grooved solid conveying zone. A uniform virgin polypropylene (PP) granule, an irregularly plate-shaped PP regrind and a powdery polyethylene (PE) are processed at screw speeds up to 1350 rpm. Thereby, frictionally engaged conveying in the grooves is visualized for the utilized powder. Similarly, the virgin granule is subject to forced conveying by interlocking in the grooves. The experimentally determined throughput is furthermore compared to analytical calculations which assume a so-called nut–screw conveying. It is found that these calculations perfectly predict the throughput when processing the virgin granule and the powder in a helically grooved barrel. In contrast, the analytical calculation significantly underestimates the throughput for the regrind. This underestimation is expected to be mainly caused by its plate shape and a difference in bulk density. The actual bulk density in the extruder is probably significantly higher due to both orientation and compaction effects compared to the measured bulk density that is used for the analytical calculation. Additionally, the regrind exhibits a fluctuating throughput due to the non-constant bulk density, which results from an irregular regrind shape and a broad size distribution.

Keywords: extrusion; solid conveying; grooved feed zone; recycled regrind; powder; virgin granule; plastics



Citation: Johann, K.S.; Reißing, A.; Bonten, C. Comparative Analysis of the Solid Conveying of Regrind, Virgin and Powdery Polyolefins in Single-Screw Extrusion. *J. Manuf. Mater. Process.* **2022**, *6*, 56. <https://doi.org/10.3390/jmmp6030056>

Academic Editor: Victor Neto

Received: 4 May 2022

Accepted: 22 May 2022

Published: 24 May 2022

Publisher's Note: MDPI stays neutral with regard to jurisdictional claims in published maps and institutional affiliations.



Copyright: © 2022 by the authors. Licensee MDPI, Basel, Switzerland. This article is an open access article distributed under the terms and conditions of the Creative Commons Attribution (CC BY) license (<https://creativecommons.org/licenses/by/4.0/>).

1. Introduction

Single-screw extrusion is a widespread and well-established processing technique in plastic industry [1–3]. Nevertheless, the process is subject to changing requirements. In addition to using well defined and uniform virgin granules, the processing of recycled, irregularly shaped regrind becomes more and more important [4–6]. This results in different conveying characteristics of the extruder.

With regard to the utilized barrel, single-screw extruders are divided into smooth and grooved set-ups. A smooth barrel extruder exhibits a backpressure-dependent throughput. In contrast to this, an extruder with a grooved solid conveying zone allows for a throughput which is independent of the backpressure, at least as long as the backpressure does not exceed a certain threshold value [7].

The conveying of plastic materials in a grooved solid conveying zone can be divided into two main cases [8]. In the first case, there is a mass flow in the grooves additionally to the usual mass flow in the screw channel. In the second case, the grooves are filled with the material but without an additional conveying in the grooves [8]. Nevertheless, the plastic filled grooves lead to a different conveying behavior, since the friction between the conveyed material to the barrel wall is modified.

There is a further subdivision of the first case into 1.(a) and 1.(b) and of the second case into 2.(a) and 2.(b) depending on the geometrical relation between the groove depth, the

granule diameter and the screw channel depth [8,9]. The case 1.(a) is supposed to take place if the groove depth is smaller than the granule diameter and if the screw channel depth is *smaller* than two times the granule diameter. The case 1.(b) is assumed to take place if the groove depth is smaller than granule diameter and if the screw channel depth is *larger* than two times the granule diameter. The case 2.(a) and the case 2.(b) are supposed to apply if the groove depth and the screw channel depth are larger, respectively significantly larger than the granule diameter [8,9]. The case 2.(a) thus applies for small granules, whereas the case 2.(b) is typically assumed for materials with very small granule size such as powder or grit. A schematic illustration of the four solid conveying cases can be found for instance in [8].

The case 1.(a) assumes a material conveying in the grooves since the moving screw flight forces a mass transport. There, the axial conveying velocity in the screw channel is expected to be equivalent to the axial conveying velocity in the grooves. This is analogous to the so-called nut–screw conveying described in [10]. The case 1.(b) also assumes a material conveying in the grooves forced by the moving screw flight. Nevertheless, a different conveying velocity is expected between the material in the grooves and the material layer in the lower screw channel region due to a slip plane formation [11]. It should be mentioned that the usual textbook assumption [8], which states that there is no solid conveying in grooves for the cases 2.(a) and 2.(b) is a simplification. It was shown that whether conveying in the grooves takes place not only depends on the geometrical relations but also on the processed material itself respectively its inner friction [11].

As described above, the geometrical relation between the groove depth, the granule diameter and the screw channel depth play an important role in the mass transport of a grooved solid conveying zone. Approaches to calculate the mass throughput \dot{m} as a function of the screw speed n in a grooved barrel extruder are primarily derived from historically preceding works on smooth barrel extruders [12–14]. Many works are based on the following linear approach, which comprises the bulk density ρ_b of the plastic granule, the extruder’s free cross-sectional area A_f that is available for mass transport, the axial conveying velocity v_{ax} of the granule as well as the filling degree f of the screw channel:

$$\dot{m} = \rho_b \cdot A_f \cdot v_{ax} \cdot f. \tag{1}$$

At low screw speeds, the filling degree can be assumed to be equal to one, since there is enough time for complete filling of the screw channel. Furthermore, effects such as a vortex formation in the hopper, which result in a partially filled screw channel [15–19], can be omitted at low screw speeds. However, if a certain threshold screw speed is exceeded, a non-linear, respectively, degressive throughput behavior is observed [20–23]. This non-linearity can then be taken into account by a screw speed-dependent filling degree which is smaller than one.

The free cross-sectional area can be subdivided into the free cross-sectional area of the screw channel A_s and into the free cross-sectional area of the grooves A_g . With regard to this further division, Equation (1) can be written as:

$$\dot{m} = \rho_b \cdot (A_s + A_g) \cdot v_{ax} \cdot f. \tag{2}$$

The free cross-sectional area of the screw channel can be calculated with:

$$A_s = \left(\frac{\pi}{4} \cdot (D_s^2 - D_c^2) - \frac{w_f}{\sin \varphi} \cdot h_s \cdot i_s \right), \tag{3}$$

where D_s is the outer screw diameter, D_c is the core diameter of the screw, w_f is the width of the flight perpendicular to the helix direction, φ is the helix angle of the screw, h_s is the screw channel depth and i_s is the number of screw flights in the cross-sectional area.

The free cross-sectional area of the grooves can be calculated using:

$$A_g = \frac{w_g}{\sin \omega} \cdot i_g \cdot h_g, \tag{4}$$

with w_g being the width of the groove perpendicular to the groove direction, ω being the groove angle, i_g being the number of grooves and h_g being the groove depth. The throughput calculations are always referred to the plane perpendicular to the extrusion direction at the end of the feed opening. For axial grooves that possess a groove angle of 90° , the $\sin \omega$ term equals to one and thus disappears. If the solid conveying angle α and the circumferential screw speed v_{circ} are known, the axial conveying velocity can be calculated [10] via:

$$v_{\text{ax}} = v_{\text{circ}} \cdot \frac{\tan \varphi}{\frac{\tan \varphi}{\tan \alpha} + 1} = \pi \cdot n \cdot D_s \cdot \frac{\tan \varphi}{\frac{\tan \varphi}{\tan \alpha} + 1} \tag{5}$$

Assuming a nut–screw conveying simplifies the calculation considerably because this allows for equating the solid conveying angle with the groove angle [10]. Thereby, a rather elaborate calculation of the solid conveying angle which is based on the acting pressure and friction forces at the granule bed can be avoided.

Due to wall effects, the bulk density of the plastic material is lower near the solid wall compared to the bulk density in the middle of a large solid bed. Thus, the actual bulk density in the extruder is lower compared to bulk density, which is usually determined at a high dumping height. To account for this phenomenon, it is possible to measure the bulk density as a function of the dumping height h_{du} . Subsequently, these values can be fitted using Equation (6) [10]. This allows us to calculate the bulk density for different dumping heights. In Equation (6), ρ_0 is the maximum bulk density at a high dumping height and h_0 is the threshold dumping height, whereby for values of $h_{\text{du}} < h_0$, the bulk density is equal to zero. Both variables A and B are dimensionless fit parameters. It should be mentioned that this approach neglects any pressure-induced compaction of the solid bed. In [24–26], a description can be found for how to additionally account for a pressure and temperature dependency by measuring the materials’ compressibility.

$$\rho_b(h_{\text{du}}) = \rho_0 \cdot \left[1 - \exp \left\{ -A \cdot \left(\frac{h_{\text{du}}}{h_0} - 1 \right)^B \right\} \right] \tag{6}$$

Utilizing these bulk density values from static measurements in order to calculate the extruder’s throughput is proper for the low screw speed range. However, it can be error-prone to a certain extent at high screw speeds due to loosening effects of the solid bed [10].

As can be seen in Figure 1, a grooved solid conveying zone can be divided into three different regions, each exhibiting a different dumping height and thus a different bulk density. The mass throughput in the screw channel \dot{m}_S can be calculated by:

$$\dot{m}_S = A_S \cdot v_{\text{ax}} \cdot [BZ \cdot \rho_{\text{ss}} + (1 - BZ) \cdot \rho_{\text{sz}}] \tag{7}$$

whereas the mass throughput in the grooves \dot{m}_g can be calculated via:

$$\dot{m}_g = A_g \cdot v_{\text{ax}} \cdot [BS \cdot \rho_{\text{zz}} + (1 - BS) \cdot \rho_{\text{sz}}] \tag{8}$$

BZ and BS are dimensionless values which resemble the proportion of non-grooved barrel and the proportion of the screw flight in the cross-section area, respectively. ρ_{ss} is the bulk density between the screw and the inner barrel diameter, ρ_{sz} is the bulk density between the screw and a groove and ρ_{zz} is the bulk density between the screw flight and the groove. The latter means that the dumping height is equal to the groove depth.

When a nut–screw conveying is assumed, the overall mass throughput is the sum of both the throughput in the screw channel and the throughput in the grooves:

$$\dot{m} = \dot{m}_S + \dot{m}_g \tag{9}$$

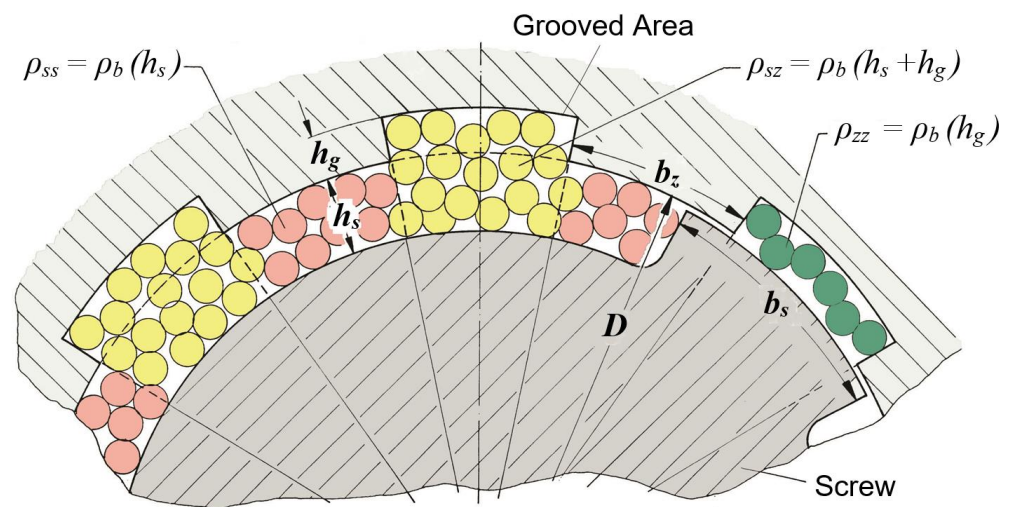


Figure 1. Schematic representation of three different areas exhibiting varying bulk densities due to different dumping heights in a grooved solid conveying zone. Drawn and kindly provided with the permission to use by E. Grünschloß (author of [10]), March, 2022.

In [27], the suitability of the linear throughput approach was examined for a grooved extruder set-up together with numerical simulations using the discrete element method (DEM). It was shown that the assumption of pressure-independent throughput is appropriate. Furthermore, it was found that the classification into the four different solid conveying cases is justified [27]. However, it is suggested that the classification should further contain the screw clearance, since the particles in the grooves will not be driven by the screw flight if the screw clearance is larger than the protrusion of the granule [27]. Moreover, it was found that the assumption of block flow is an oversimplification in certain cases [27].

Regarding the influence of particle shape on the solid conveying behavior, it was found that a small spherical granule exhibits a later onset of non-linear throughput compared to larger lenticular and cylindrical granules [28]. Furthermore, [28] shows that the throughput of a helically and an axially grooved barrel converge at high screw speeds. In [29], long cylindrical granules are compared to virgin spherical granules. Despite exhibiting a lower bulk density in measurements, the long cylindrical granule results in a higher throughput compared to the virgin spherical granule. This is explained by a forced orientation of the long cylindrical granule in the extruder, which results in a higher bulk density in the screw channel and thus a higher throughput for the long cylinders [29].

A similar effect is purposely exploited in [30,31] to achieve a higher bulk density for regrind. To enable a complete convergence of the specific throughput of virgin granules and regrind, a new solid conveying compression zone is examined there both experimentally and simulatively via DEM. To account for the irregular plate-like shape of the regrind, the DEM was conducted by utilizing superquadrics instead of spheres [30,31].

The concept of a circular economy [32] becomes more and more important due to an increasing environmental awareness among the population. This is accompanied by an increasing amount of processing recycled regrind in industry. However, there is still a severe lack of investigations that deal with the solid conveying characteristics of plastic regrind, especially in grooved single-screw extruders at high screw speed.

Thus, the aim of this work is to examine and compare the conveying characteristics of three distinctly different material shapes thoroughly. The investigated polyolefins are an irregularly plate-shaped regrind polypropylene (PP), a uniform virgin PP and a powdery polyethylene (PE). All materials are processed with a smooth and a helically as well as an axially grooved solid conveying zone at screw speeds up to 1350 rpm. To investigate whether a well-established analytical approach is also suitable for regrind, the experimentally determined throughput is compared to these analytical predictions. Furthermore, the solid conveying is optically observed by using transparent poly(methyl

methacrylate) (PMMA) barrels. The new findings of this work can thus be utilized in the future as a starting point to improve the extruder's machine and process design, particularly when processing plastic regrind.

2. Materials and Methods

2.1. Used Materials and Characterization of the Geometrical Dimensions and Bulk Density

Three different polyolefins were chosen, since they are frequently processed in an industry with extruders that possess a grooved solid conveying zone. The three materials primarily differ with regard to their particle shape. As a virgin lenticular granule, *Moplen EP440G* from the company LyondellBasell, Rotterdam, the Netherlands was used, which is a polypropylene (PP) copolymer for extrusion blow molding applications. The regrind material was a PP exhibiting a plate-like shape. Since this material was previously used in an industrial flat-sheet extrusion process, the exact material composition and specifically its tradename is unknown. The chosen powdery plastic is *Lupolen 5461 B Q471*, which is a high-density polyethylene (PE) from the company LyondellBasell, Rotterdam, the Netherlands, that can be used for the extrusion of peroxide crosslinked pipes. The different plastic shapes are schematically depicted in Figure 2 and labeled with the geometric dimensions. Pictures of the three materials can be found in Figure 3.

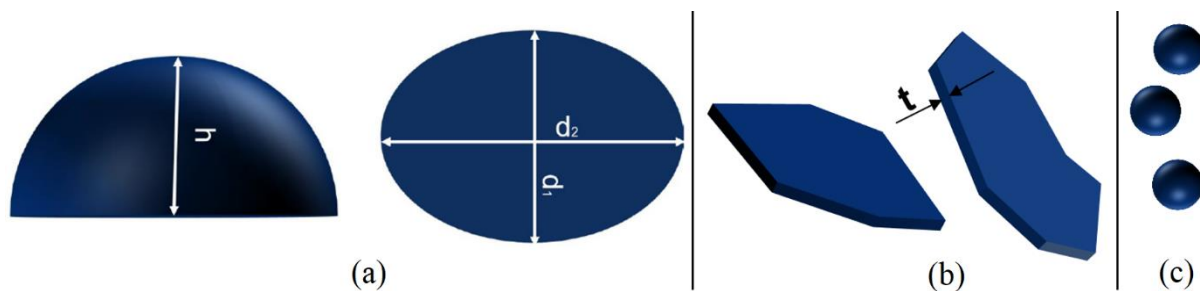


Figure 2. Schematic representation of (a) the lenticular virgin PP, (b) the irregularly shaped regrind PP and (c) the powdery PE.

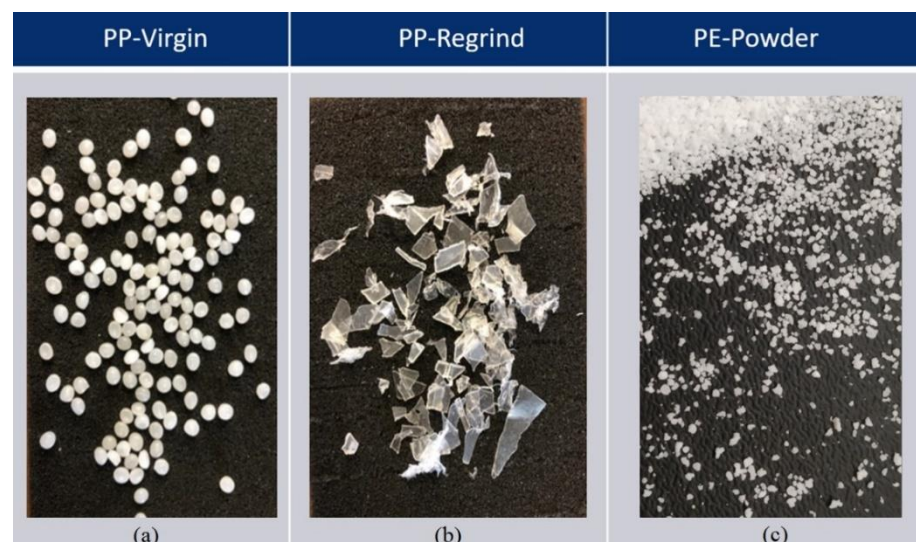


Figure 3. Pictures of (a) the virgin PP granule (b) the regrind PP (c) the powdery PE.

The projected area of the virgin granule and of the regrind material was determined using a flatbed scanner *Perfection V850 Pro* from the company Seiko Epson Corporation, Suwa, Nagano, Japan. The two-dimensional scans were quantitatively analyzed using the open-source software *Fiji ImageJ*. It was necessary to manually separate individual particles on the scanner surface in order to obtain a proper analysis.

The virgin PP material was characterized with regard to both of its diameters d_1 , d_2 and its height h with 200 measurements for each dimension. The mean value of d_1 is $3.55 \text{ mm} \pm 0.14 \text{ mm}$, the mean value of d_2 is $4.10 \text{ mm} \pm 0.19 \text{ mm}$ and h possesses a mean value of $1.98 \text{ mm} \pm 0.18 \text{ mm}$. The mean projected area of the virgin PP is 12.4 mm^2 with a relative standard deviation of 8% (see Figure 4a). Hence, the virgin material shows a very narrow respectively homogeneous granule geometry and size distribution.

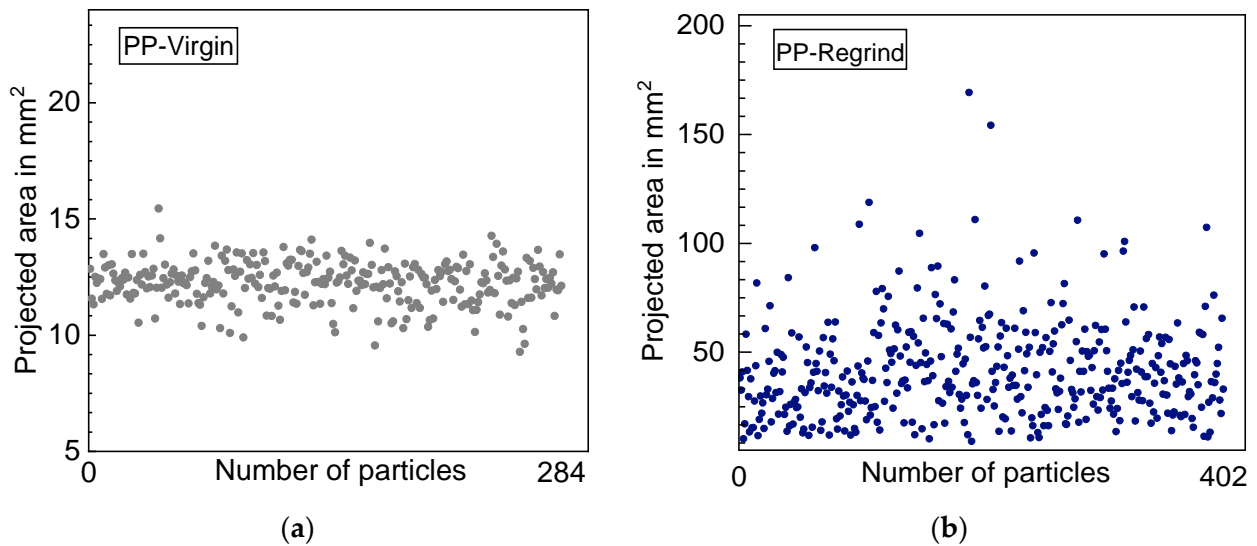


Figure 4. Projected area of (a) the virgin PP granule (b) the regrind PP material determined by using a flatbed scanner.

The regrind PP material was examined with regard to its particle thickness t for 100 different flakes. The mean thickness amounts to $0.46 \text{ mm} \pm 0.37 \text{ mm}$. The mean projected area is 42.3 mm^2 with a large relative standard deviation of 54%, as can be seen in Figure 4b. The large deviations in particle thickness as well as in the projected area make clear that the regrind material exhibits a very inhomogeneous particle shape (see Figure 3) and size (see Figure 4).

The powdery PE possesses a nominal 25 mesh size according to its data sheet which corresponds to approximately $725 \mu\text{m}$ particle size. Further geometrical measurements were omitted in this case. This is due to the small particle size which made quantitative analysis by means of the flatbed scanner or a manual determination of the particle dimensions difficult and error-prone.

The bulk density was determined as a function of dumping height. To do so, a measuring cup with a 50 mm diameter and a height adjustable bottom was utilized, analogous to the proceeding described in [10]. The dumping height was varied between 2 and 20 mm in 2 mm steps. Furthermore, a dumping height of 50 mm was used following DIN EN ISO 60 [33]. The measurements were repeated three times for each dumping height.

The respective results are shown in Figure 5, whereby the utilized materials exhibit an increasing bulk density with increasing dumping height and subsequently converge to a maximum value. In all three cases, the standard deviation is considerably higher for the lower dumping heights (<10 mm). Furthermore, the regrind material exhibits a higher standard deviation for intermediate dumping heights (10–20 mm) compared to the virgin and powdery plastic. The results of fitting the measured data with Equation (6) can be found in Table 1. The respective fitting functions were used to calculate the bulk density for the three different dumping heights of 2.8 mm (for ρ_{zz}), 5.5 mm (for ρ_{ss}) and 8.3 mm (for ρ_{sz}), which exist in the utilized grooved solid conveying zone (see the geometrical information given in Table 2). In contrast, only one dumping height respectively bulk density (ρ_{ss}) exists in the smooth barrel solid conveying zone.

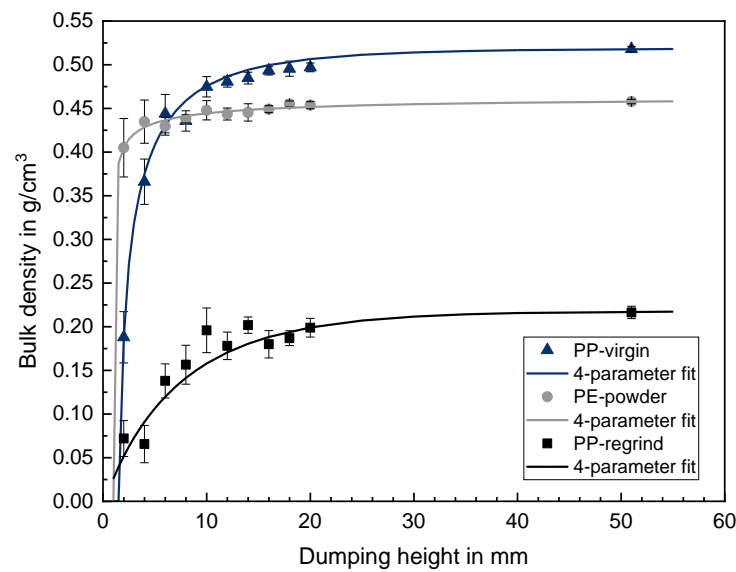


Figure 5. Bulk density measurements for increasing dumping height and respective 4-parameter-fits for the virgin PP, the regrind PP and the powdery PE.

Table 1. Bulk density fit parameter as well as the calculated bulk density values for the three different areas in the grooved solid conveying zone.

Granule	Bulk Density Fit Parameter				Bulk Density		
	ρ_0 in g/cm ³	h_0 in mm	A (Dimensionless)	B (Dimensionless)	ρ_{zz} (2.8 mm) in g/cm ³	ρ_{ss} (5.5 mm) in g/cm ³	ρ_{sz} (5.5 mm) in g/cm ³
PP-Virgin	0.519	1.698	1.095	0.518	0.303	0.420	0.462
PP-Regrind	0.218	0.230	0.042	0.914	0.069	0.113	0.144
PE-Powder	0.463	1.047	2.122	0.193	0.419	0.435	0.442

Table 2. Geometrical dimensions of the utilized screw and of the helically and the axially grooved barrel (data from [28]).

Geometry Parameters	Dimension
Outer screw diameter D_s	34.85 mm
Core diameter of the screw D_c	23.85 mm
Helix angle of the screw φ	17.73°
Screw channel depth h_s	5.5 mm
Width of the screw flight w_f	3.5 mm
Number of screw flights i_s	1
Width of a groove w_g	5.5 mm
Groove angle ω	41.19° (helical) 90° (axial)
Groove depth h_g	2.8 mm
Number of grooves i_g	6 (helical) 10 (axial)

2.2. Experimental Set-Up of the Mere Solid Conveying Zone and of the Entire Extruder

The solid conveying behavior was investigated using three different water-cooled solid conveying zones with an overall length of 300 mm and an inner barrel diameter of 35 mm. With this set-up, melting of the plastic material is avoided, and free granule

trickling without additional backpressure at the end of the solid conveying zone is enabled. One steel barrel had six helical grooves and another steel barrel had ten axial grooves. Furthermore, one smooth steel barrel was used as a reference. Both grooved barrels exhibit a continuous groove depth of 2.8 mm below the 80 mm long feed opening. Subsequently, the groove depth runs out to zero until the end of the solid conveying zone. Other relevant geometrical information of the utilized screw and of the grooved barrels can be found in Table 2.

The free cross-sectional area of the screw channel was calculated by Equation (3) and amounts to 443.8 mm² for all three barrels. Employing Equation (4) leads to a free cross-sectional area of the grooves, which is 140.2 mm² for the helical grooves and 154 mm² for the axial grooves. In terms of the total free cross-sectional area, which is the sum of A_s and A_g , the helically and the axially grooved barrel purposely show a similar total free cross-sectional area, which only differs by approximately 2%. Thus, differences in throughput between both of the grooved solid conveying zones are primarily caused by a different axial conveying velocity. The values of BZ and BS contained in Equations (7) and (8) are $BZ = 0.623$ and $BS = 0.105$ for the helically grooved barrel as well as $BZ = 0.578$ and $BS = 0.105$ for the axially grooved barrel.

The throughput was measured for screw speeds between 50 and 1350 rounds per minute (rpm, whereas its unit is equal to 1/min). This corresponds to a circumferential screw speed of 0.09–2.47 m/s. The freely trickling granule was collected for 45 s at the respective screw speed and subsequently weighed. For each type of material and each barrel type, two independent series of experiments were conducted, exhibiting a high reproducibility with a maximum relative deviation of 2–3% for the virgin PP as well as for the powdery PE and of 5–8% for the regrind PP.

In order to observe the solid conveying, especially with regard to an expected mass transport in the grooves, transparent duplicates of the three steel barrels were manufactured using poly(methyl methacrylate) (PMMA). The transparent PMMA barrels were only used for optical observation without conducting throughput measurements because they possess different friction conditions between the processed material and the barrel wall. The helically grooved PMMA solid conveying zone was plugged into a surrounding steel casing with two observation windows, as can be seen in Figure 6. The recorded videos of processing the different materials with the grooved transparent PMMA barrels can be made available on e-mail request (see Supplementary Materials).

As a third experimental set-up, an entire 100 kW extruder with an axial length of 1190 mm (35/34D) was used. The screw had an outer screw diameter of 34.85 mm, and the screw clearance amounts to 0.15 mm. This set-up exhibited a helically grooved solid conveying zone that is equal to the mere helically grooved solid conveying zone previously described. The entire extruder furthermore consisted of a smooth barrel in the melting and in the metering zone as well as a throttle die at the end. This set-up allows comparing the throughput of a real extrusion process to the throughput of the mere solid conveying zone. A schematic drawing of the utilized set-up can be found in [23]. The screw and barrel were manufactured by the company Helix GmbH, Winnenden, Germany, and the throttle die was built by the company Keller, Ihne & Tesch KG, Lampertheim, Germany. This set-up included an additional melting of the processed plastics. The screw is designed like a classical barrier screw [34] and thus with an additional screw flight in the melting zone. The screw geometry in the solid conveying zone is equivalent to the previously screw geometry that was used in the solid conveying experiments. At the end of the screw, a spiral shearing device and a Saxton mixer were additionally used as a combined mixing element to improve melt homogenization. The throttle die facilitated the precise regulation of the die backpressure and was varied between 50 and 200 bar. The respective pressure profile over the extruder length depended on the processed material, the screw speed and the adjustable die backpressure. The pressure always exhibited a continuously decreasing profile in extrusion direction which is typical for systems with a grooved solid conveying zone (see [23]). For instance, the pressure in the beginning of the melting zone

was around 650 bar for 150 rpm and 50 bar die pressure when processing the virgin PP. The pressure and temperature profiles were measured by using five combined pressure and temperature sensors at different axial positions from the DTAI series from the company Gneuß Kunststofftechnik GmbH, Bad Oeynhausen, Germany. The respective signals were processed and recorded using LabVIEW from the company National Instruments, Austin, Texas, USA. The helically grooved solid conveying zone was cooled by means of water to a temperature of approximately 60 °C. The melting and the metering zone as well as the die were always heated up to 230 °C, whereas the barrel was heated via four heating elements and the throttle die was heated via six heating elements. The actual temperature for regulating the respective heating elements was measured by type J thermocouples.



Figure 6. Experimental set-up using a helically grooved PMMA barrel.

3. Results

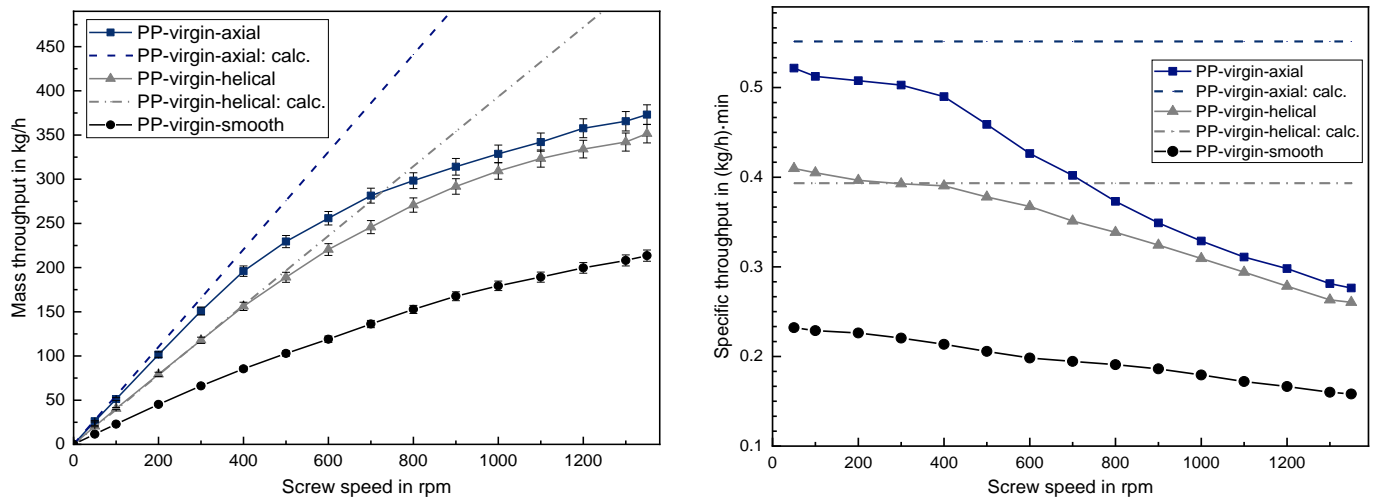
The mass throughput is always predicted by using Equations (7)–(9). This includes the throughput in the screw channel according to Equation (7) and the throughput in the grooves according to Equation (8). Since a nut-screw conveying is assumed, the solid conveying angle is supposed to be equivalent to the groove angle, which is 41.19° for the helically grooved case and 90° for the axially grooved case. This is purposely created at this point without a further discrimination into the four different solid conveying cases. A detailed discussion hereto is found in the proceeding work. The three different bulk densities (ρ_{ss} , ρ_{sz} and ρ_{zz}) for each material are given in Table 1 and the free cross-sectional area of the screw channel and of the grooves are given in Section 2.2.

The results of the analytical calculation are subsequently always depicted as dashed lines. Calculating the throughput when utilizing the smooth barrel is omitted because the governing friction coefficients were not determined. Examining the specific throughput, which is the throughput per screw rotation (calculated via \dot{m}/n), makes it easier to evaluate the start of non-linear throughput behavior as well as to compare the values of different material shapes among each other.

3.1. Virgin PP Granule—Results of the Measured, Calculated and Observed Solid Conveying

The results of the mass throughput determination when using the virgin PP granule are shown in Figure 7. The three series of experiments exhibit a linear throughput behavior at low screw speeds. This is followed by a pronounced degressive behavior when exceeding approximately 300 rpm. At low screw speeds, the axially grooved barrel results in a specific throughput of around 0.51 (kg/h) min and the helically grooved barrel in around 0.40 (kg/h) min. This can be attributed to the higher axial conveying velocity when using the axially grooved solid conveying zone. Nevertheless, the axial grooves lead to a steep

decline in throughput when exceeding 300 rpm. Thus, a slow converge of throughput between the axial and the helical grooves can be observed by increasing screw speed.



(a)

(b)

Figure 7. (a) Mass throughput and (b) specific mass throughput for the virgin PP granule.

Regarding the prediction quality of the analytical approach, the calculated throughput perfectly matches with the measured throughput when utilizing the helically grooved barrel. The mean relative deviation between the calculated and the measured values is approximately 2% at 50–300 rpm in this case. This finding underlines the importance of taking the bulk density as a function of the dumping height into account in order to obtain appropriate throughput predictions.

Contrary to this, the calculation overestimates the throughput in the axially grooved case with a mean relative deviation of approximately 7% at 50–300 rpm. This behavior can be explained by taking the results of an optical observation into account.

Figure 8a shows a picture of processing the virgin PP with a helically grooved PMMA barrel. Figure 8b depicts the virgin PP in an axially grooved PMMA barrel. In both cases, the screw speed was successively increased from 10 to 100 rpm at maximum in order to avoid frictional wear of the PMMA barrels. It is observed that in the helically grooved case the virgin PP granule perfectly satisfies the assumptions of a nut–screw conveying. The rotating screw flight forces a solid conveying in the grooves due to the protrusion of the virgin PP out of the grooves. Furthermore, a perfect block flow is observed both in the grooves and in the fully filled screw channel. Thereby, the solid conveying angle is equivalent to the groove angle for the entire solid bed.

In contrast, for the axially grooved barrel, it is observed that the assumptions of a nut–screw conveying are not fulfilled. This results in a certain deviation between the predicted and the measured throughput. Both the assumption of block flow and the assumption that the solid conveying angle in the screw channel is equivalent to the groove angle do not hold in this case. A relative movement between individual PP particles in the screw channel is observed, particularly in the vicinity of the screw flight. This deviation from block flow is caused by the friction of the PP granule to the rotating screw flight. This results furthermore in a deviation from the supposed 90° solid conveying angle. Thus, the real solid conveying angle in the screw channel is somewhat lower. Furthermore, it should be mentioned that an adequate block flow is only observed in the axially grooved barrel at the lowest screw speed of 10 rpm. The relative movement between individual PP granules in the screw channel became more pronounced with increasing screw speed. This eventually lead to the case that PP granules which were entrapped in the axial grooves

could escape the grooves. Thus, even a mass exchange between the axial grooves and the screw channel was observed for the virgin PP granule by increasing screw speed.

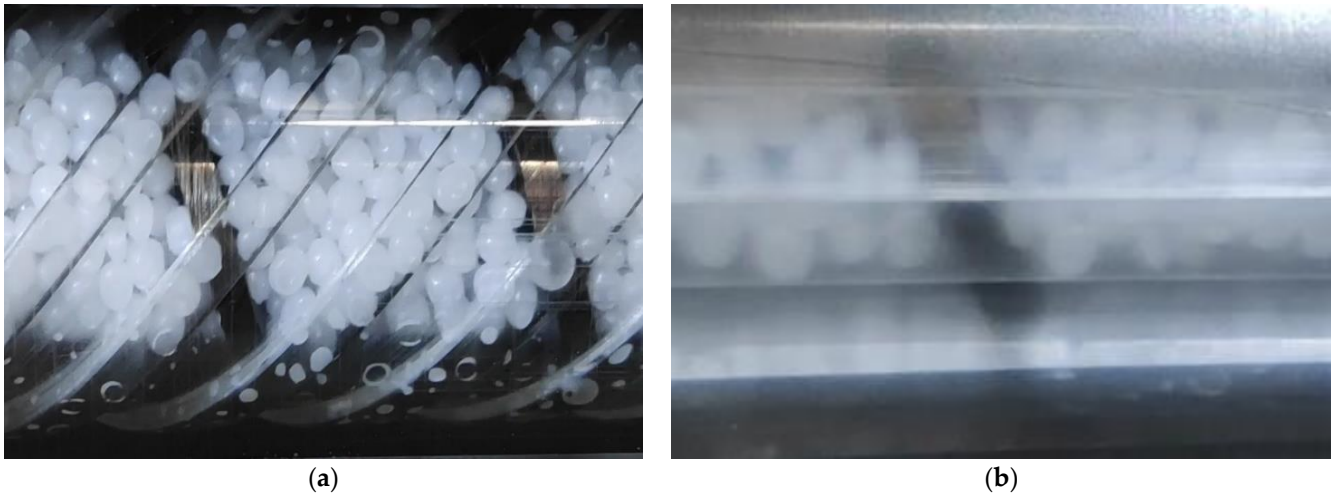


Figure 8. Virgin PP granule processed with a transparent PMMA barrel exhibiting (a) helical grooves (b) axial grooves.

3.2. Regrind PP Flakes—Results of the Measured, Calculated and Observed Solid Conveying

The results of measuring the mass throughput for the regrind PP can be found in Figure 9. In contrast to the virgin PP, the regrind PP already exhibits a decreasing specific throughput at low screw speeds, especially for both grooved solid conveying zones. The specific throughput is highest for the axially grooved barrel with values slightly above 0.20 (kg/h)·min, followed by the helically grooved barrel with values around 0.18 (kg/h)·min regarding the low screw speed range of 50–300 rpm. There, the smooth barrel also exhibits a low specific throughput of around 0.11 (kg/h)·min.

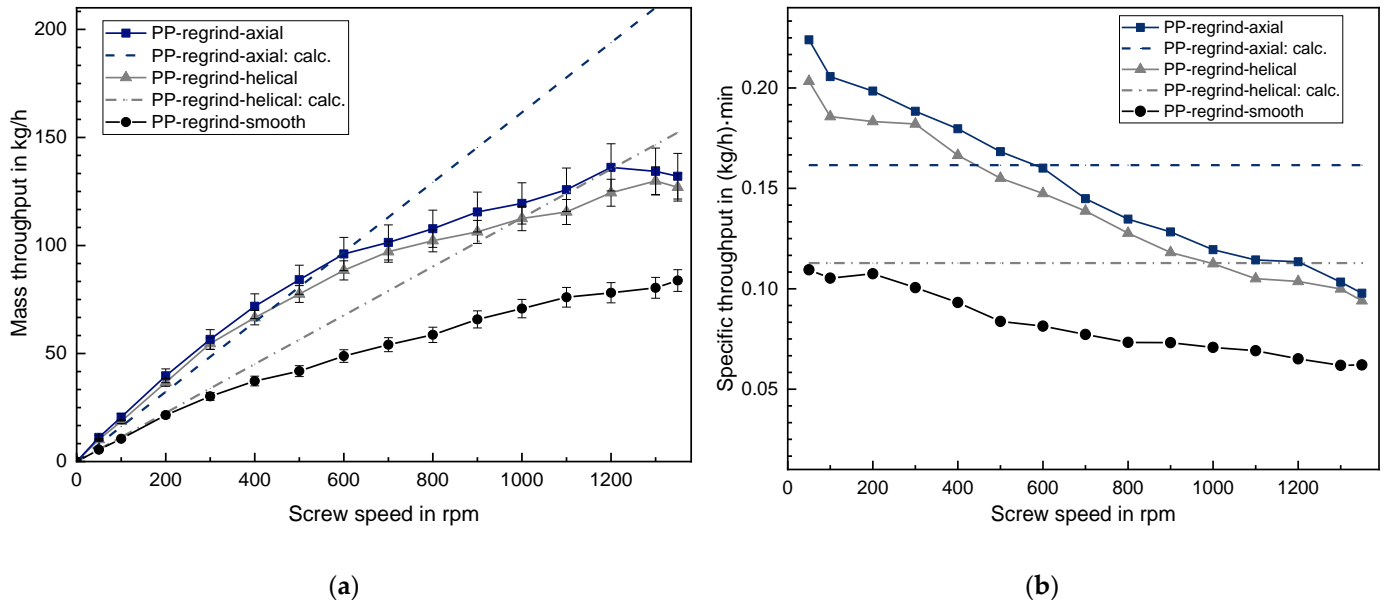


Figure 9. (a) Mass throughput and (b) specific mass throughput for the regrind PP material.

Moreover, the throughput for both grooved barrels is already very similar at low screw speeds when processing the regrind PP. This is accompanied by a relatively high deviation between independent series of experiments which is approximately 4–7%. This is accompanied by large error bars in Figure 9a. The high deviation between different series of experiments is primarily caused by the irregular regrind shape and its broad size

distribution. This results in an inhomogeneous and non-constant bulk density and thus a fluctuating mass throughput, which is contrary to the steady respectively constant bulk density when using virgin PP.

The quality of throughput prediction for both grooved systems is very poor for the regrind PP, even in the helically grooved case. The calculation significantly underestimates the measured values with a mean relative deviation of 67% for the helically grooved barrel and a mean relative deviation of 26% for the axially grooved barrel, even at the low screw range between 50 and 300 rpm.

This large deviation is expected to be primarily caused by the circumstance that the regrind's bulk density in the extruder is probably considerably higher than the measured bulk density, which is used for the calculations due to a compression effect as well as an orientation effect. On the one hand, [31,35] revealed that regrind exhibits a substantially higher compressibility than virgin granules. This means that the bulk density of regrind increases faster when applying a certain pressure, in particular in the low-pressure regime [35]. On the other hand, a resembling effect was observed in [29] for long cylindrical granules due to a forced orientation in the extruder, which leads to a higher bulk density and thus a higher mass throughput than expected. A similar orientation behavior is conceivable for the utilized plate-shaped regrind that displays a large aspect ratio as well.

An optical investigation of the solid conveying behavior of the regrind PP was unfortunately not possible. Processing the regrind in a smooth PMMA barrel lead to a melting of the regrind even at a very low screw speed of 10 rpm. This melting lead to damage of the barrel's inner surface and a significant deterioration of the optical transparency. This is because the plate-shaped regrind exhibited a very high heat generation due to plastic–plastic friction, which could not be removed fast enough due to the low thermal conductivity of the PMMA barrel. Since using a grooved barrel leads to even higher friction, the axially and helically grooved PMMA barrel were not used for processing the regrind in order to avoid damage to these barrels.

3.3. Powdery PE Particles—Results of the Measured, Calculated and Observed Solid Conveying

The results of measuring the mass throughput for the powdery PE are depicted in Figure 10. The respective measurements show a very low deviation between independent series of experiments in each case, which results in small error bars. The specific throughput at low screw speeds between 50 and 300 rpm is around 0.43 (kg/h) min for the axially grooved barrel, around 0.40 (kg/h) min for the helically grooved barrel and approximately 0.21 (kg/h) min for the smooth barrel.

In contrast to the previous results of virgin PP and regrind PP, the powdery PE exhibits a linear throughput behavior even at high screw speeds. Utilizing the helically grooved barrel results in a linear throughput up to 700 rpm. The throughput behavior for the smooth barrel even remains linear until the maximum screw speed of 1350 rpm. Thus, the powdery PE exhibits a beneficial trickling behavior out of the hopper opening into the screw channel, which ensures a fully filled screw channel even at high screw speeds.

The fully filled screw channel is also verified optically up to 1000 rpm by means of the smooth PMMA barrel. Higher screw speeds were omitted in this case to avoid too high frictional wear at the PMMA barrel's inner surface. This observation for the powdery PE is in good accordance with previous observations in [28], which showed a similar advantageous behavior when processing a small and spherical polyamide (PA) granule.

Regarding the quantitative values, the throughput of the powdery PE is already quite close in the low screw speed range for both the axially and the helically grooved barrel. Furthermore, the calculation precisely predicts the throughput up to 700 rpm for the helically grooved barrel. As opposed to this, the calculation considerably overestimates the throughput for the axially grooved barrel.

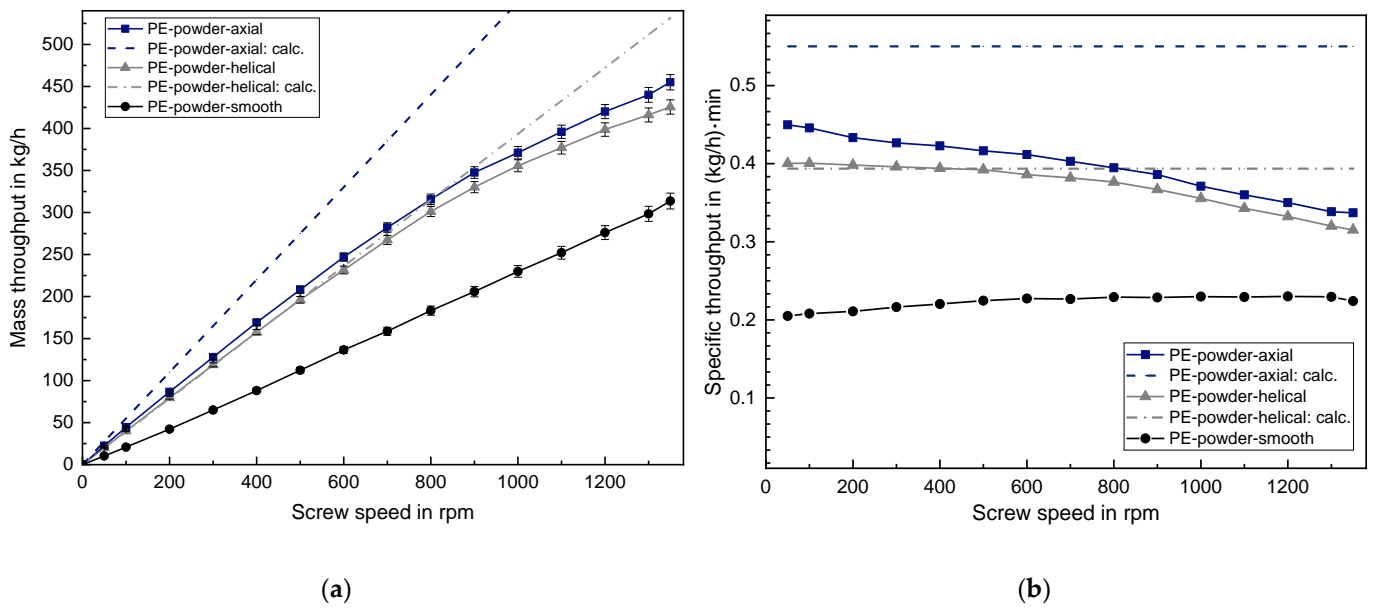


Figure 10. (a) Mass throughput and (b) specific mass throughput for the powdery PE material.

In order to account for this observation, the throughput is predicted for both systems, once using a calculation that assumes an additional mass transport in the grooves (see Equations (7)–(9)) and once using a calculation that only considers a mass transport in the screw channel (see Equation (7)). Figure 11a shows that assuming a nut–screw conveying and hence an additional mass transport in the grooves is necessary to obtain a proper throughput prediction for the helically grooved barrel. Otherwise, the calculation vastly underestimates the measured values. As can be seen in Figure 11b, this behavior is the other way around for the axially grooved barrel. There, the calculation that considers an additional conveying in the grooves overestimates the measured throughput. Contrary, the calculation that neglects additional conveying in the grooves is in good accordance with the measured values. Nevertheless, by means of using an axially grooved PMMA barrel, the latter observation is proven to be coincidentally caused by a superposition of two opposing effects.

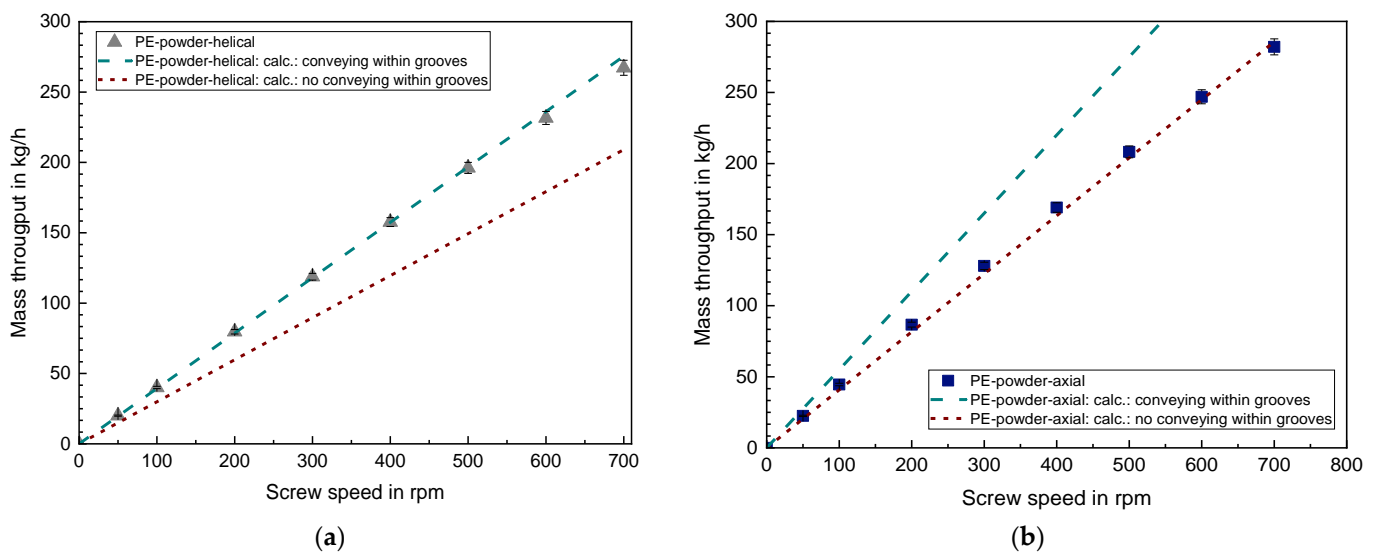


Figure 11. Comparison of the measured throughput for the powdery PE to the calculated throughput (a) for the helically grooved and (b) for the axially grooved barrel.

Pictures of processing the powdery PE in a helically and an axially grooved PMMA barrel are shown in Figure 12a,b, respectively. For the helically grooved PMMA barrel, a proper nut–screw conveying is observed. Specifically, the powdery PE exhibits a quasi-ideal block flow. Furthermore, a mass conveying in the grooves is observed, whereby both the powder in the grooves and in the screw channel exhibit a solid conveying angle that is equal to the groove angle. This explains the good agreement between the measured and the calculated throughput in this case.

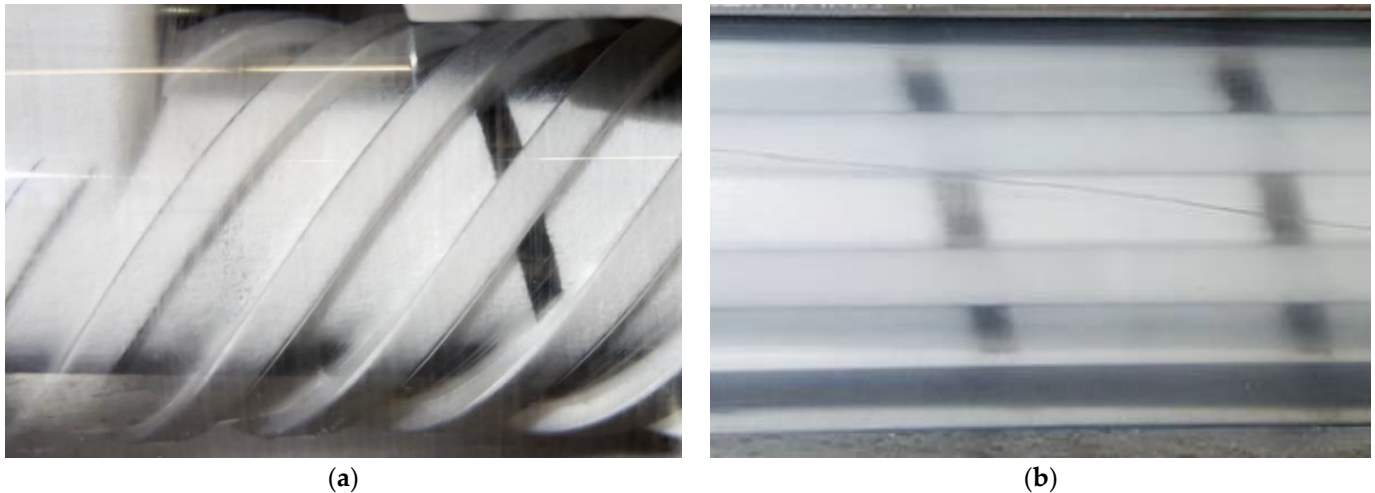


Figure 12. Powdery PE processed with a transparent PMMA barrel exhibiting (a) helical grooves, (b) axial grooves.

Another important finding is that the general assumption that there is no mass conveying in the grooves for the solid conveying case 2.(b) [8] is an inappropriate simplification. This result confirms a previous work [11], which declared that conveying in grooves depends not only on the geometrical relations but also on the processed material itself. Thus, the inner friction of the used PE powder is so high that a frictionally engaged conveying takes place in the grooves. The reason for this frictionally engaged conveying is thus different to the forced interlocking conveying (solid conveying case 1.(a)), which was observed for the virgin PP granule in this work.

Compared to the preceding observation, the powdery PE does not fully satisfy a nut–screw conveying for the axially grooved barrel. There, the solid conveying angle in the screw channel is lower than the 90° groove angle. Nevertheless, it is revealed that there is a mass conveying in the grooves but with a slower conveying velocity than the powder in the screw channel. This dragging behind of the powder in the grooves is accompanied by a slip plane formation, and hence, the block flow assumption is not accurate in this case.

3.4. Results of the Entire Extruder Set-Up Compared to the Mere Solid Conveying Zone

The throughput results of using an entire extruder set-up with a helically grooved solid conveying zone and additionally a melting and metering zone with a smooth barrel are shown in Figure 13a for the virgin PP and in Figure 13b for the powdery PE. For both materials, an increasing throttle die pressure does not lead to a reduction in throughput due to the backpressure-independent behavior of these grooved extruder set-ups.

For the virgin PP, the throughput of the mere helically grooved solid conveying zone is nearly identical to the throughput of the entire extruder set-up. There, the maximum relative deviation amounts to 2.6% at a screw speed of 300 rpm, which can be attributed to a small uncertainty of measurement.

In the case of powdery PE, the values of the mere solid conveying zone exhibit a somewhat higher deviation to the values of the entire extruder set-up. The relative deviation is between 2.9 and 7.2%. Hence, the previously shown throughput results of

using a mere grooved solid conveying zone can be transferred very well to entire extruder set-ups. It should be kept in mind that this does not apply for smooth barrel systems.

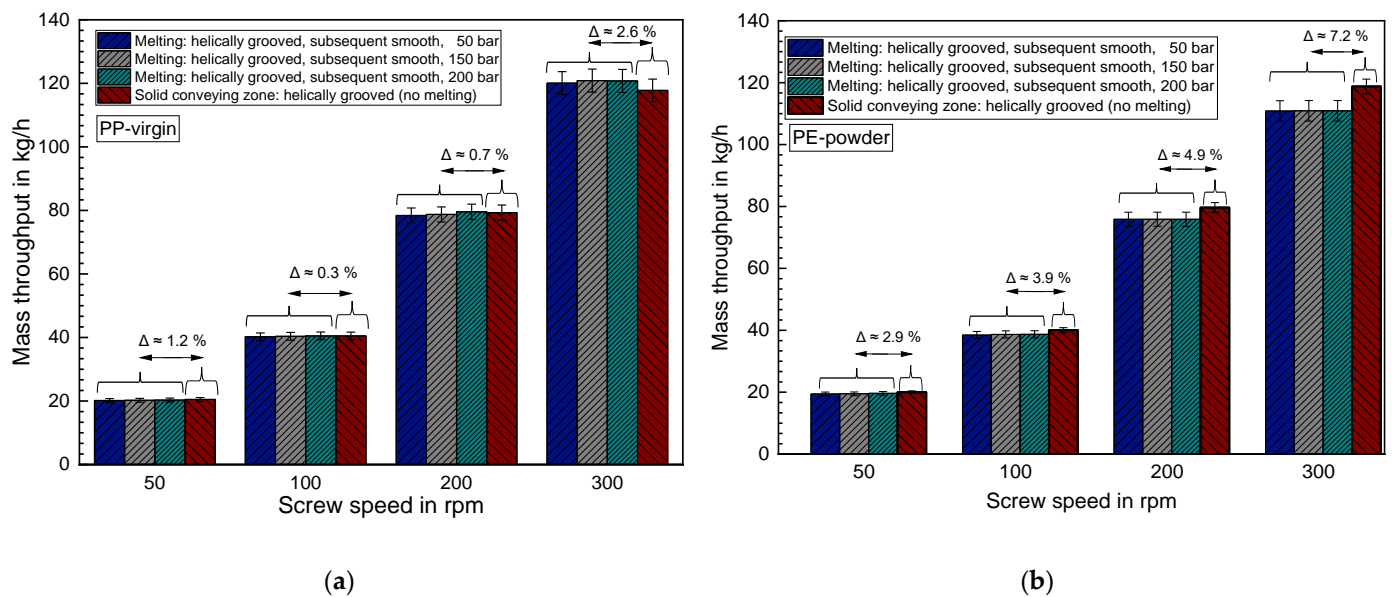


Figure 13. Comparison of the mass throughput in a whole extrusion set-up at different throttle pressures to the throughput in a mere helically grooved solid conveying zone (a) for the virgin PP and (b) for the powdery PE.

4. Conclusions

4.1. Conclusions

This study investigated the solid conveying behavior of three distinctly different plastic shapes in a smooth as well as an axially and a helically grooved solid conveying zone up to 1350 rpm. For the uniform virgin PP granule, the determined throughput perfectly matches with the analytical calculations in the helically grooved case. Since the virgin PP satisfies the conditions of the solid conveying case 1.(a), a forced mass conveying in the grooves could be visualized using a transparent PMMA barrel. Contrary to this, it is optically observed that both the assumption of block flow as well as the assumption that the solid conveying angle is equal to the groove angle do not hold in the axially grooved case. This leads to an overestimation of the calculated throughput in this latter case.

Similar results are obtained for the powdery PE, namely a precise match between calculated and measured throughput for the helical grooves and an overestimation for the axial grooves. Moreover, it is shown that a frictionally engaged conveying in the grooves takes place despite that the powder satisfies the conditions of the solid conveying case 2.(b). For the helically grooved barrel, a perfect nut–screw conveying and thus block flow is observed. As opposed to this, the axially grooved barrel exhibits a slip plane formation within the conveyed powder. This leads to a slower conveying velocity in the grooves compared to the conveying velocity in the screw channel. Furthermore, the powdery PE displays a beneficial trickling behavior. This results in a fully filled screw channel even at high screw speed. The latter effect leads to a linear mass throughput of powdery PE up to 700 rpm when utilizing the helically grooved barrel and even up to 1350 rpm for the smooth barrel.

The regrind PP results in a significantly different solid conveying behavior than both materials previously described. There, optical observations using a PMMA barrel were not possible due to a very high frictionally generated heat which led to melting. Furthermore, the throughput measurements exhibit a very large deviation between repeated series of experiments. This is attributed to the irregular regrind shape and its broad size distribution. Both aspects lead to a non-constant bulk density and thus a fluctuating throughput. The analytical calculation underestimates the regrind throughput for both the axially and the

helically grooved barrel substantially. This is predominantly attributed to both orientation and compaction effects, which result in a higher bulk density in the extruder compared to the measured bulk density, which is used for the calculation.

4.2. Outlook

In order to obtain a reasonable analytical throughput prediction for plastic regrind, its compressibility must be considered in future work in order to account for an increasing bulk density due to the acting pressure in the extruder. Furthermore, the issues of a non-constant bulk density as well as a low specific throughput still have to be solved for regrind. One approach of how to partly overcome these issues by means of an adapted extruder design can be found in [30,31].

Supplementary Materials: Available online at <https://bwsyncandshare.kit.edu/s/tDERFZg4amQXm5p>, accessed on 20 May 2022. The recorded videos of processing the virgin PP and the powdery PE with the grooved transparent PMMA barrels can be made available on e-mail request.

Author Contributions: Conceptualization, K.S.J.; methodology, K.S.J.; formal analysis, A.R. and K.S.J.; investigation, A.R. and K.S.J.; data curation, K.S.J.; writing—original draft preparation, K.S.J.; writing—review and editing, K.S.J., A.R. and C.B.; visualization, K.S.J. and A.R.; supervision, C.B.; project administration, K.S.J. and C.B.; funding acquisition, C.B. All authors have read and agreed to the published version of the manuscript.

Funding: This research was funded by the Deutsche Forschungsgemeinschaft (DFG, German Research Foundation) with grant number: BO 1600/56-1, project number: 423276016).

Institutional Review Board Statement: Not applicable.

Informed Consent Statement: Not applicable.

Data Availability Statement: Not applicable.

Acknowledgments: Special thanks go to the Helix GmbH (Winnenden, Germany) for providing two transparent PMMA barrels free of charge and for the fruitful cooperation in several extrusion projects and to T. Molter for supporting the extrusion experiments.

Conflicts of Interest: The authors declare no conflict of interest. The funders had no role in the design of the study; in the collection, analyses, or interpretation of data; in the writing of the manuscript, or in the decision to publish the results.

References

1. Wortberg, J.; Haberstroh, E.; Lutterbeck, J.; Masberg, U.; Schmidt, J.; Targiel, G. Designing of extrusion lines. *Adv. Polym. Technol.* **1982**, *2*, 75–106. [CrossRef]
2. Carneiro, O.S.; Ferrás, L.L.; Teixeira, P.; Fernandes, C.P.; Nóbrega, J.M. Weld Lines in Extrusion: Understanding the Role of the Flow Conditions. *AIP Conf. Proc.* **2015**, *1662*, 030012. [CrossRef]
3. Rajkumar, A.; Ferrás, L.L.; Fernandes, C.; Carneiro, O.S.; Becker, M.; Nóbrega, J.M. Design Guidelines to Balance the Flow Distribution in Complex Profile Extrusion Dies. *Int. Polym. Proc.* **2017**, *32*, 58–71. [CrossRef]
4. Reich, M.J.; Woern, A.L.; Tanikella, N.G.; Pearce, J.M. Mechanical Properties and Applications of Recycled Polycarbonate Particle Material Extrusion-Based Additive Manufacturing. *Materials* **2019**, *12*, 1642. [CrossRef]
5. Karaagac, E.; Jones, M.P.; Koch, T.; Archodoulaki, V.-M. Polypropylene Contamination in Post-Consumer Polyolefin Waste: Characterisation, Consequences and Compatibilisation. *Polymers* **2021**, *13*, 2618. [CrossRef]
6. Běhálek, L.; Novák, J.; Brdlík, P.; Borůvka, M.; Habr, J.; Lenfeld, P. Physical Properties and Non-Isothermal Crystallisation Kinetics of Primary Mechanically Recycled Poly(l-lactic acid) and Poly(3-hydroxybutyrate-co-3-hydroxyvalerate). *Polymers* **2021**, *13*, 3396. [CrossRef]
7. Bonten, C. *Plastics Technology—Introduction and Fundamentals*; Hanser Publisher: Munich, Germany, 2019; ISBN 979-1-56990-767-2.
8. White, J.L.; Potente, H. *Screw Extrusion: Science and Technology*; Hanser Publishers: Munich, Germany, 2003; ISBN 978-3-446-19624-7.
9. Schöppner, V. *Process Engineering Design of Extrusion Lines*; Progress Reports VDI No. 715; VDI Verlag: Düsseldorf, Germany, 2001; ISBN 3-18-371503-1. (In German)
10. Grünschloß, E. Bulk density and mass throughput in grooved barrel extruders. *Kunststoffe* **1993**, *83*, 309–311.
11. Potente, H.; Schöppner, V. A Throughput Model for Grooved Bush Extruders. *Int. Polym. Proc.* **1995**, *4*, 289–295. [CrossRef]
12. Schneider, K. The Conveying Process in the Feed Zone of an Extruder. Ph.D. Thesis, Rheinisch-Westfälische Technische Hochschule Aachen, Aachen, Germany, 1968.

13. Schneider, K. The influence of the feed zone on the conveying characteristics of a single-screw extruder. *Kunststoffe* **1969**, *59*, 757–760.
14. Goldacker, E. Investigation of the Internal Friction of Powders, Particularly Regarding Conveying in Extruders. Ph.D. Thesis, Rheinisch-Westfälische Technische Hochschule Aachen, Aachen, Germany, 1971.
15. Pohl, T.C. Development of High-Speed Single Screw Systems for Plastics Processing Based on Basic Theoretical Investigation. Ph.D. Thesis, Universität Paderborn, Fakultät für Maschinenbau, Paderborn, Germany, 2003.
16. Moysey, P.A.; Thompson, M.R. Investigation of solids transport in a single-screw extruder using a 3D discrete particle simulation. *Polym. Eng. Sci.* **2004**, *44*, 2203–2215. [[CrossRef](#)]
17. Leßmann, J.S.; Weddige, R.; Schöppner, V.; Porsch, A. Modelling the solids throughput of single screw smooth barrel extruders as a function of the feed section parameters. *Int. Polym. Proc.* **2012**, *27*, 469–477. [[CrossRef](#)]
18. Leßmann, J.-S. Calculation and Simulation of Solids Conveying Processes in Single-Screw Extruders up to the High-Speed Range. Ph.D. Thesis, Fakultät für Maschinenbau, Universität Paderborn, Paderborn, Germany, 2016.
19. Potente, H.; Pohl, T.C. Polymer Pellet Flow out of the Hopper into the First Section of a Single Screw. *Int. Polym. Proc.* **2002**, *1*, 11–21. [[CrossRef](#)]
20. Trippe, J.; Schöppner, V. Modeling of solid conveying pressure throughput behavior of single screw smooth barrel extruders under consideration of backpressure and high screw speeds. *Int. Polym. Proc.* **2018**, *33*, 486–496. [[CrossRef](#)]
21. Roth, M. High-Speed Single Screw Extruders: State of Development. In *Extrusionstechnik 2010: Hochleistungsextrusion und Betriebskostenoptimierung*; VDI Wissensforum GmbH, VDI-Gesellschaft Kunststofftechnik: Bonn, Germany, 2010; pp. 21–32.
22. Kast, O.; Bonten, C. Investigation of a High-speed Extruder with a Helically Grooved Melting Zone. *J. Plast. Technol.* **2015**, *3*, 180–203.
23. Kast, O.; Bonten, C. Influence of a Grooved Melting Zone on High-speed Single Screw Extrusion. *AIP Conf. Proc.* **2016**, *1779*, 03004. [[CrossRef](#)]
24. Peiffer, H. Contribution to the Conveying Problem in the Grooved Feed Zone of Single-Screw Extruders. Ph.D. Thesis, Rheinisch-Westfälische Technische Hochschule (RWTH), Fakultät für Maschinenwesen, Aachen, Germany, 1981.
25. Hwang, C.-G.; McKelvey, J.M. Solid Bed Compaction and Frictional Drag During Melting in a Simulated Plasticating Extruder. *Adv. Polym. Technol.* **1989**, *9*, 227–251. [[CrossRef](#)]
26. Hyun, K.S.; Spalding, M.A.; Hinton, C.E. Theoretical and Experimental Analysis of Solids Conveying in Single-Screw Extruders. *J. Reinf. Plast. Compos.* **1997**, *16*, 1210–1219. [[CrossRef](#)]
27. Brüning, F.; Schöppner, V. Numerical Simulation of Solids Conveying in Grooved Feed Sections of Single Screw Extruders. *Polymers* **2022**, *14*, 256. [[CrossRef](#)]
28. Johann, K.S.; Mehlich, S.; Laichinger, M.; Bonten, C. Experimental Investigation of the Solid Conveying Behavior of Smooth and Grooved Single-Screw Extruders at High Screw Speeds. *Polymers* **2022**, *14*, 898. [[CrossRef](#)]
29. Längauer, M.; Liu, K.; Kneidinger, C.; Schaffler, G.; Purgleitner, B.; Zitzenbacher, G. Experimental analysis of the influence of pellet shape on single screw extrusion. *J. Appl. Polym. Sci.* **2015**, *132*, 41716. [[CrossRef](#)]
30. Thieleke, P.; Bonten, C. Enhanced Processing of Re grind as Recycling Material in Single-Screw Extruders. *Polymers* **2021**, *13*, 1540. [[CrossRef](#)] [[PubMed](#)]
31. Thieleke, P. Increasing the Process Window of Single-Screw Extruders Operated with Re grind as Recycling Material. Ph.D. Thesis, Fakultät für Energie-, Verfahrens- und Biotechnik, Universität Stuttgart, Stuttgart, Germany, 2020.
32. Neto, V. Eco-design and Eco-efficiency Competencies Development in Engineering and Design Students. *Educ. Sci.* **2019**, *9*, 126. [[CrossRef](#)]
33. *Deutsche Fassung EN ISO 60:1999*; Determination of the Apparent Density of Molding Compounds That Can Flow through a Standardized Funnel (Bulk Density)—ISO 60:1977. Deutsches Institut für Normung e. V. Kunststoffe: Berlin, Germany, 2000.
34. Wortberg, J. Screw concepts for high-performance extrusion—Barrier screws. In *The Single Screw Extruder—Fundamentals and System Optimization*; Wortberg, J., Fischer, P., Eds.; Verein Deutscher Ingenieure VDI-Gesellschaft Kunststofftechnik: Düsseldorf, Germany, 1997; pp. 139–163. ISBN 3-18-234203-7.
35. Langecker, G.R. Investigating the Behaviour of Plastic Powders in the Feed Zone of Single-Screw Machines with Grooved Bushes. Ph.D. Thesis, RWTH Aachen University, Aachen, Germany, 1977.